Early infection of *Phytophthora agathidicida* up-regulates photosynthetic activity in *Agathis australis* seedlings

K. D. D'Souza[1*], P. Scott[2], N. Williams[2], S.E. Bellgard[3], and M. K.-F. Bader[1, 4]

[1] Auckland University of Technology, 34 St Paul Street, Auckland 1010, New Zealand

[2] The New Zealand Institute for Plant and Food Research Limited, New Zealand

[3] Massey University, Palmerston North, New Zealand

[4] Current address: Swiss Federal Institute for Forest, Snow and Landscape Research, Zürcherstrasse 111, 8903 Birmensdorf, Switzerland

*Corresponding author: Kimberley D'Souza,

Auckland University of Technology,

34 St Paul Street,

Auckland 1010,

New Zealand.

Email: kim_d@hotmail.co.nz

This document is the accepted manuscript version of the following article:
D'Souza, K. D., Scott, P., Williams, N., Bellgard, S. E., & Bader, M. K. F. (2021). Early infection by Phytophthora agathidicida up-regulates photosynthetic activity in Agathis australis seedlings. Forest Pathology. https://doi.org/10.1111/efp.12680

Abstract

New Zealand kauri (*Agathis australis*) trees are culturally, socially and ecologically significant within northern New Zealand's nutrient-poor podocarp forest ecosystems. *Phytophthora agathidicida* is an aggressive oomycete pathogen, capable of killing *A. australis* across its ecological range, causing the disease known as kauri dieback. The pathogen, like many other forest *Phytophthora* species, commences as a fine root rot which progresses to collar rot and resinous cankers on the lower trunk. In this study, we investigated the eco-physiological and fine root responses of kauri to infection by *P. agathidicida* and tested whether the foliar application of micronutrients (manganese and zinc combined, iron alone, or a trace element mix) affects dieback disease expression. Fortnightly assessments of chlorophyll-*a*-fluorescence were conducted over 12 weeks, and fine root length and tip numbers were recorded at the end of the experiment. None of the micronutrient treatments had a significant physiological effect regardless of pathogen infection. However, contrary to expectations, pathogen infection caused a significant upregulation in photosynthetic activity over time, as the electron transport rate of infected plants was approximately 26 % higher than that of control plants at the end of the trial. These results indicate that an increase in the strength of the below-ground carbon sink through pathogen consumption of labile carbohydrates (sugars), together with pathogen-induced root damage, triggered upregulation of photosynthesis in the seedlings. Understanding how *P. agathidicida* infection affects the physiology and resource allocation in kauri is critical to determining the disease aetiology and management options.

Key words: kauri dieback, remote sensing, micronutrient amendments, plant pathogens, root rot, leaf spectral signatures

Word Count: 243

Introduction

Kauri (*Agathis australis* (D.Don) Lindl.*)* has ecological, historical and cultural value to both indigenous and non-indigenous New Zealanders (Steward & Beveridge, 2010). Consequently, the decline of this species is having significant negative impacts on the already heavily fragmented kauri population (National (Kauri Dieback) Pest Management Plan, 2019). *Phytophthora* species are notorious invasive plant pathogens that have spread into new environments, where the hosts have little natural resistance, through globalisation and the movement of infected organic material (Bae et al., 2016; Scott, Bader, Burgess, Hardy & Williams, 2019).

In New Zealand, 32 described species of *Phytophthora* with known host species have been identified (Manaaki-Whenua Landcare Research, 2020). Four of these species, *Phytophthora agathidicida, P. cinnamomi*, *P. multivora* and *P. cryptogea,* are all associated with dieback in *A. australis* (Waipara, Hill, Hill, Hough & Horner, 2013); however, only *P. agathidicida* has been identified as the primary causal agent of kauri dieback disease (Horner & Hough, 2014). Three other *Phytophthora* species occur in kauri forest soils: *P. chlamydospora, P. nicotianeae* and *P. kernoviae* (Scott & Williams, 2014), but to date none of these species has been associated with disease dieback in *A. australis*.

Similar to the majority of *Phytophthora* pathogens*, P. agathidicida* starts by infecting the fine roots of *A. australis*, then progresses further into the plant through the larger roots parasitising the cambium (Shilton, 2017; Bellgard, Pennycook, Weir, & Waipara, 2016). The pathogen infects the living tissue consuming available sugars and nutrients, undermining the tree's physiological resilience and eventually killing the tree (Bellgard, Probst, Padamsee, Williams, & Weir, 2019). The infection progresses to the root collar of the tree forming a canker that exudes resin, causing vascular dysfunction inhibiting water and nutrient uptake (Shilton, 2017; Bellgard et al., 2016). These symptoms represent the chronic phases of the disease but *P. agathidicida* probably infects the fine roots many years before above-ground symptoms become visible (Bradshaw et al., 2020).

Kauri trees have considerable physiological resilience conferred through their longevity, immense size and interconnection with the environment around them. This physiological resilience is a key factor in understanding the ability of kauri to ward off infection – the conditions under which these trees will succumb to infection and the time taken for trees to decline in the presence of *P. agathidicida*.

Understanding the impact of *P. agathidicida* on kauri physiology is therefore fundamental to understanding disease latency and expression within forest systems.

As with many coniferous plants, *A. australis* can form root anastomoses that result in a grafted root network amongst neighbouring trees, allowing the quick exchange of water and nutrients (Bader & Leuzinger, 2019). While these root connections may help buffer the effects of abiotic stressors through re-allocation of resources, they also provide a pathway for rapid pathogen transmission among members of a grafted root system further complicating conservation efforts to control the spread of kauri dieback disease (Bader & Leuzinger, 2019). *Agathis australis* makes efficient use of what little nitrogen and phosphorus is available in kauri forests through arbuscular mycorrhiza aided nutrient acquisition and litter recycling (Wyse, Burns, & Wright, 2014; Padamsee et al., 2016). However, biomass and nutrition studies of *A. australis* in a 130-year-old stand in the Hunua Ranges (Madgwick, Oliver, & Holten-Anderson, 1982) confirmed earlier work of Peterson (1963) indicating that the availability of both nitrogen and phosphorus are limiting to *A. australis* growth.

Although resistance to plant diseases is generally dependent on genetics, nutrient availability is known to have a significant effect on the tolerance and resistance of plants against various diseases, both positively and negatively (Nadeem, Asif Hanif, Mejeed, & Mushtaq, 2018). For example, high nitrogen concentration increased the susceptibility of potatoes to foliar infection by *P. infestans* (Mittelstraß et al., 2006). However, the role of nutrient availability on host resilience to infection by *P. agathidicida* has yet to be investigated, together with the direct and indirect physiological consequences of the disease. In addition to challenges through a paucity of macronutrients, specific micronutrients are vital in ensuring the proper growth and development of plants as well as playing a significant role in plant defence and the incidence and/or severity of diseases (Rengel, 1999). The structural and catalytic role of metal micronutrients in many enzymes is crucial for disease resistance and tolerance in plants (Graham & Webb, 1991). Nutrient manipulation through soil drenches, fertilisation, foliar sprays, and/or systemic nutrient implants has widely been used to improve plant health and subsequently reduce the severity of diseases (Nadeem et al., 2018). The severity of plant disease can be inferred from impacts upon key eco-physiological traits (Rolfe & Scholes, 2010), such as the electron transport rate of photosystem II (ETR, a proxy for photosynthesis), which are sensitive to root and vascular dysfunction.

Measurements of chlorophyll fluorescence are widely used in plant pathological research as an indicator of pathogen-related biotic stress affecting the photosynthetic metabolism of plants (Rolfe & Scholes, 2010). For example, Schnabel, Strittmatter, & Noga. (1998), detected physiological impairment of potato cultivars as early as 48 hours after infection with *Phytophthora infestans* based on chlorophyll fluorescence recordings. Similarly, Manter, Kelsey, & Karchesy. (2007) used a chlorophyll fluorescence approach to investigate the physiological impacts of *P. ramorum* infection on *Rhododendron macrophyllum* and found that the photosynthetic capacity of inoculated plants decreased by approximately 21 % in the first three weeks. Likewise, Scharte, Schön, & Weir. (2005) reported an overall decrease in photosynthetic electron transport (PET) in tobacco leaves in response to infection with *P. nicotianae* using chlorophyll fluorescence imaging. However, Horsfall & Diamond. (1957) have previously explained of a phenomenon known as “high sugar resistance,” whereby biotic stressors, including pathogen infection, trigger an increase in sugar production as part of a defence mechanism in infected plants. The authors describe that there is a close linkage between plant carbohydrate-status and the outcome of a plant-pathogen interaction. High sugar levels intensify the oxidative burst typically seen in the early stages of plant infection, boost cell wall lignification and prompt the sugar-dependent activation of many pathogen-related defence compounds such as flavonoids (Morkunas & Ratajczak, 2014).

This study aimed to investigate the physiological response of kauri seedlings to early infection by *P. agathidicida* and the potential role of plant micronutrients in the development of kauri dieback. To date, there have been no studies investigating the role of micronutrient application influence on the photosynthetic response of *A. agathis* infected with *P. agathidicida.* In a glasshouse seedling trial, we tested the hypotheses that:

i) infection of kauri seedlings with *P. agathidicida* causes a significantly decline in the photosynthetic capability of the host;

ii) micronutrient addition improves the resilience and tolerance of *A. australis* to infection by *P. agathidicida*;

iii) a mixed micronutrient treatment application to *A. australis* seedlings is more effective than individual micronutrient application.

Materials and Methods

Experimental design

The study was laid out as a stratified randomised split-plot design comprising five whole blocks, with 'seed family' as a whole-plot factor, '*P. agathidicida* infection' as a subplot factor and 'micronutrients' as sub-sub plot factors. Each block contained 48 plants divided between infected and uninfected (control) plants, with 16 individuals from each of the three families. The treatment variables were pathogen infection (*P. agathidicida* and control consisting of sterile millet without *P. agathidicida*), micronutrient addition (no addition, zinc & manganese, iron, and a mixed complement of micronutrients) and seed family (A, B, C). The *post hoc* measured variables were presence/absence of infection, root assessment (root length and root tip number) and chlorophyll fluorescence.

The experiment was conducted in a glasshouse at the Manaaki Whenua - Landcare Research facility in St Johns, Auckland, New Zealand, under a Consent to Operate (CTO) approval for the communication and propagation of the "unwanted organism", *P. agathidicida*. In total, 240 kauri seedlings from three different families (A,B,C) were sourced from Te Roroa, Waipoua, Northland, in consultation with local iwi, and grown at the Scion nursery (Rotorua, New Zealand, -38.1578 S, 176.2686 E) under strict nursery hygiene required to prevent contamination by *Phytophthora* pathogens. All seedlings were approximately 2.5 years of age with heights ranging from 20 to 58 cm. Seedlings were removed from their original soil and re-potted using the same pots, into sterilized (autoclaved) river sand. Seedlings and pots were thoroughly washed, using reverse osmosis (RO) water, to ensure any soil residue was removed. Prior to the start of the experiment, seedlings were acclimatised to the new environment for two weeks.

The *P. agathidicida* isolate NZFS-3813 (ICMP 21138) used in this study was isolated from soil under *A. australis* in Whangaparoa (Coromandel region) in 2014 and sourced from the New Zealand Forest Service Mycological Collection. The inoculum was prepared by growing isolate NZFS-3813 for 7-days on V8® juice agar plates at 18°C. Fifteen, 6 mm plugs of agar were removed from the advancing edge of the cultures. The colonised agar plugs were placed into autoclaved white millet seeds (300 mL), which were thoroughly moistened with V8® juice (Campbell Soup Company, United States) (Vettraino, Natili, Anselmi, & Vannini, 2001). The flasks were incubated at 20°C for six weeks. The control millet

inoculum was prepared by adding clarified buffered V8 broth to 300 mL of white millet seed. The uninoculated millet was incubated at 20°C for six weeks (Vettraino et al., 2001; Jeffers, 2006).

A week prior to inoculation, 25 seeds from the inoculated and control millet flasks were plated to P_5ARPH selective media (Jeffers, 2006), to confirm the viability of the inoculated millet and confirm that the control-millet was pathogen-free.

Root inoculation

Two weeks after repotting, infested millet was added to the inoculated pots while non-inoculated, sterile millet was added to the control pots. The top 2 cm of river sand was gently removed to expose the collar of the stem, and 5 g of millet seed was added, after which the sand was replaced in the pot. Following inoculation, all pots were flooded with reverse osmosis (RO) water to the top of the trays to induce sporulation. After 48 hours, the trays were drained. Plants were housed in a glasshouse with a temperature that ranged between 18°C and 21°C and watered every 4 days with 100 mL of RO water per plant. Six weeks into the experiment, the pots were all re-flooded for 48 hours and then re-drained, to re-induce sporulation. To confirm sporulation, 200 mL water samples recovered from the inoculated pots, were baited with 10 Himalayan Cedar needles (*Cedrus deodara* (Roxb.) G.Don), for 48 hours. The baits were removed from the water, surface disinfested in 70% ethanol for 30 seconds, then rinsed in de-ionised water, dried between clean paper towels, before being plated onto P_5ARPH selective media and incubated for at 18°C for 4-7 days. The underside of the agar plates were scanned under a Nikon Ni compound microscope (Nikon Corporation, Kanagawa, Japan) to confirm the presence of oospores of *P. agathidicida* being produced from the colonised cedar needle baits.

Micronutrient treatments

Micronutrient solutions were applied to plants two weeks following millet inoculations. The micronutrients used in this study were commercially available systemic micronutrient formulations (Table 1). The commercially recommended rate of 32 mL of each micronutrient was added to 1 L of RO water, then sprayed onto the foliage of the seedlings. The control for the foliar nutrient application

consisted of spraying 1 L of RO water onto the control seedlings. To prevent contamination of the soil, the seedlings were spatially separated during application of each of the foliar treatments.

Re-application of nutrients was done every two weeks following the same method as described above, using the set concentration of 32 mL of each micronutrient treatment. All pots were placed on drip trays to avoid cross-contamination between the respective inoculation and nutrient treatments.

Table 1: Composition and application amount of micronutrient treatments, iron, zinc and manganese and a mixed treatment (DuluxGroup Pty Ltd, Yates New Zealand).

Micronutrient treatment	**Volume applied (within 1 L of RO water)**	**Treatment constituents**
Yates Chelated Iron Liquid ™	32 mL	Iron (Fe) as iron lignosulfonate chelate 1.25 % w/v
Yates Citrus Cure Zinc & Manganese ™	32 mL	Zinc (Zn) as zinc lignosulphonate chelate 1.25 % w/v Manganese (Mn) as lignosulphonate chelate 1.25 % w/v
Yates Trace Elements Liquid ™	32 mL	Sulphur (S) as sulphate 0.53 % w/v Iron (Fe) as iron lignosulphonate chelate 0.34 % w/v Magnesium (Mg) as magnesium lignosulphonate chelate 0.34 % w/v Zinc (Zn) as zinc lignosulfonate chelate 0.34 % w/v Manganese (Mn) as manganese lignosulphonate chelate 0.26 % w/v Boron (B) as boron lignosulphonate chelate 0.13 % w/v Copper (Cu) as copper lignosulphonate chelate 0.043 % w/v Molybdenum (Mo) molybdenum lignosulphonate chelate 0.005 % w/v

Physiological health measurements

Rapid light response curves of electron transport rate (ETR) of photosystem II were recorded using a pulse amplitude-modulated fluorometer (Mini-PAM, Walz, Effeltrich, Germany) to determine the saturating light intensity (photosynthetic photon flux density, PPFD) for subsequent chlorophyll-*a*-

fluorescence measurements. The light curves were fitted using a generalised nonlinear least-squares regression approach (R package *nlme,* Pinheiro et al., 2018), based on the following equation:

$$ETR = ETR_{max} \cdot (1 - \exp(- \alpha \cdot PPFD / ETR_{max}))$$

where ETR_{max} is the maximum ETR and α is the initial slope (quantum efficiency at low PPFD). The light curve analysis indicated that light saturation at 90 % of ETR_{max} occurred at approximately 400 µmol m^{-2} s^{-1}. Subsequent chlorophyll-*a*-fluorescence measurements aimed at determining the maximum ETR were carried out at approximately 600 µmol m^{-2} s^{-1} to ensure full light saturation. Three leaves, in total, were chosen from the top, middle and bottom sections of each seedling. Photosystem II efficiency (yield) and the ETR were recorded. Chlorophyll fluorescence was measured before the addition of micronutrients, and then every two weeks until the end of the experiment (12 weeks in total).

Statistical analysis

The statistical analyses of the electron transport rate (ETR) and root data were performed in R (3.6.1, R Development Core Team, 2018).

Analysis of Electron Transport Rate (ETR)

The analysis of the maximum electron transport rates (ETR) was conducted using a linear mixed-effects model (R function, *lme*), as a function of pathogen treatment (control, infected), micronutrients (Control, Fe, Mn + Zn, Mixed), seed family (A, B, C) and the time following nutrient application (1 – 12 weeks) and their interactions (R package, *nlme,* Pinheiro et al., 2018). The nesting structure of the random term in descending order was: block (1 – 5), pathogen treatment, micronutrients and seed family. Model assumptions of variance homogeneity and normality of the residuals were examined through model diagnostic plots (residuals vs fitted values, normal Quantile – Quantile (Q-Q) plot). The diagnostic plots for the ETR data indicated slight violations of the variance homogeneity and normality assumptions. Variance heterogeneity was modelled using a constant variance per stratum variance function with ‘week’ as grouping variable (R function *varIdent*) resulting in residual plots without violations of the variance homogeneity or normality assumptions. The optimal variance modelling

approach was determined by comparing different variance structures using the Akaike Information Criterion (AIC).

A backward selection procedure based on likelihood ratio tests was used to identify which explanatory variables were significant. *Post hoc* comparisons using Tukey contrasts were performed to follow up on significant interactions (R-package *emmeans*, Lenth, 2019). Statistical significance was determined at $\alpha = 0.05$.

Analysis of root data

The root length data were analysed using a linear mixed-effects model, as a function of pathogen treatment (control, infected), micronutrients (Control, Fe, Mn + Zn, Mix), seed family (A, B, C) and their interactions. The nested random term specified in the model had the descending nesting of the block (1 – 5), pathogen treatment, micronutrients and seed family (R package *nlme,* Pinheiro et al., 2018). Root lengths of less than or equal to 2 mm diameter were defined as fine roots and considered in the analysis. These were then separated into four different diameter classes: < 0.5 mm, 0.5 – <1.0 mm, 1.0 – < 1.5 mm and 1.5 – 2.0 mm. Model assumptions of variance homogeneity and normality were assessed using graphical model validation tools as described above. The diagnostic plots for root lengths that fell into the < 0.5 mm diameter category indicated slight violations in the variance homogeneity and violations of the normality assumptions. AIC-based comparisons of different variance structures identified a power of variance function using the fitted values as variance covariate as best suited for modelling the heteroscedasticity.

The number of root tips were analysed using a generalised linear mixed model with a template model builder approach using a binomial error distribution and the default logit link (R package *glmmTMB*, Brooks et al., 2017). Root tip number was expressed as a proportion per diameter category and then analysed as a function of pathogen treatment (control, infected), micronutrients (Control, Fe, Mn + Zn, Mixed), seed family (A, B, C) and their interactions. The random term was identical to those in the models above. Graphical data exploration revealed a pattern only for the number of root tips on roots < 1 mm diameter, and therefore only those were considered for statistical analysis. The proportions of root tips that fell into the < 0.5 mm and 0.5 – <1 mm diameter categories were calculated by dividing

the number of root tips in the respective diameter category by the total number of root tips observed in a seedling root system.

For both the root length and root tip number models, a backward selection procedure based on likelihood ratio tests was conducted to identify which explanatory variables were significant. Following that, a *post hoc* comparison test, using Tukey contrasts, was performed (R-package *emmeans*, Lenth, 2019). Statistical significance was determined at $\alpha = 0.05$.

Harvesting of roots

Twelve weeks after pathogen inoculation the seedlings were harvested and their roots were sliced into small fragments, surface sterilised in 70 % ethanol for 30 seconds, then rinsed in de-ionised water before being plated onto P_5ARPH selective media (pimaricin, ampicillin, rifampicin, pentachloronitrobenzene and hymexazol) (Jeffers, 2006). The plates were then incubated at 20 °C, checked after 7 days for emergent colonies and reassessed at 11 days to confirm the presence of *P. agathidicida.*

The harvested roots were scanned to determine treatment impacts by measuring root length and root tip number. All plants were removed from the river sand, washed thoroughly in RO water and spread in a water bath for imaging on a flatbed scanner. Images were then analysed using WinRhizo™ (Regent Instruments Inc., Québec, Canada).

Results

Impact of infection and nutrient application on electron transport rate

Neither the four-way interaction (pathogen × micronutrients × family × assessment week) nor any of the three-way interactions were statistically significant, although the treatment interaction of pathogen × micronutrients × week was marginally significant ($p = 0.052$; Table 2). Among the two-way interactions only pathogen × week was statistically significant, indicating that pathogen infection affected ETR, depending on the time after inoculation (Table 2; Figure 1). Seed family also had a significant effect on the ETR of plants (Table 2), where inoculated seedlings of family A, B and C caused roughly a 5 %, 12 % and 4.5 % increase in ETR, respectively, compared with the uninoculated seedlings (Figure 1). To emphasize the pathogen × week interaction, we display its

effect size as the difference in ETR between control and the inoculated plants, pooled over micronutrient treatments and seed families, in Figure 2. A *post hoc* comparison, slicing the pathogen × week interaction, revealed that significant differences occurred at nine and eleven weeks after inoculation with *P. agathidicida* (Figures 1 and 2), when infected plants showed 10 % and 16 % higher ETR respectively compared with the uninoculated control plants. Even though the 95 % confidence interval of the inoculation-related difference in ETR did not include zero at week 7 (Figure 2), this difference turned out to be insignificant after the multiplicity adjustment involved with the *post hoc* procedure. Therefore, pathogen-infection caused an overall statistically significant increase in ETR of 26 % by the end of the experiment (inclusive of weeks nine and eleven). Within seed families, statistically significant differences occurred between family A and family C, where the ETR of family A was approximately 10 % higher than that of family C.

Table 2: Results of a backwards selection procedure applied to a linear mixed effects model for the electron transport rate (ETR) data from *Agathis australis* under various treatments. The pathogen is *Phytophthora agathidicida.* Treatments are described in the text.

Dropped term	*L*	*Df*	*p*
Round #1			
Pathogen × micronutrients × seed family × week	15.63	30	0.985
Round #2			
Pathogen × micronutrients × week	24.79	15	0.052
Pathogen × micronutrients × seed family	2.98	2	0.810
Micronutrients × seed family × week	17.28	2	0.969
Round #3			
Pathogen × seed family	2.93	2	0.230
Micronutrient × seed family	10.84	6	0.093
Seed family × week	2.85	10	0.985

Pathogen × micronutrients	2.08	3	0.555
Pathogen × week	22.20	5	< 0.001 ***
Micronutrients × week	19.30	15	0.197
Round #5			
Pathogen × week	21.85	5	< 0.001***
Seed family	6.63	2	0.036 *
Micronutrients	1.67	3	0.643
Round # 6			
Seed family	6.62	2	0.036 *
Pathogen × week	21.77	5	< 0.001 ***

Note: L = likelihood ratio statistic, *Df* = degrees of freedom of the likelihood ratio statistic, *p* = *p* value.
* $p < 0.05$, *** $p < 0.001$.

Statistical significance was determined at $\alpha = 0.05$.

Impact of infection and nutrient application on root length and root tip number

The majority of the root lengths were distributed among the fine roots < 2.0 mm diameter, particularly in the < 1.0 mm diameter category (Figure 3). For the < 0.5 mm and 0.5 – <1.0 mm diameter roots, there was a significant seed family × pathogen × micronutrient interaction ($p = 0.004$ and 0.011, respectively; Table 3). There was no significant seed family × pathogen × micronutrient three-way interaction, and of the two-way interactions observed for the 1.0 – < 1.5 mm and 1.5 – 2.0 mm diameter root lengths, only the pathogen × micronutrient term was significant ($p = 0.0002$ and 0.0007, respectively; Table 3).

For the < 0.5 mm diameter roots, slicing the three-way interaction identified a significant difference between the micronutrient treatments within seed families A and C. In seed family A, the roots of uninoculated seedlings showed similar lengths, regardless of micronutrient treatment, whereas roots of inoculated seedlings receiving the Mn + Zn addition were at least 50 % shorter than seedling roots in the remaining micronutrient treatments (Figure 3A). For seed family C, uninoculated seedlings receiving the mixed micronutrient treatment had root lengths which were on average 2.5 times longer than roots of uninoculated control seedlings as well as inoculated seedlings without micronutrient addition and those treated with the Mn + Zn formulation (Figure 3A). Similar plant-family specific

differences occurred within seed families B and C for the 0.5 – <1.0 mm diameter root lengths. For seed family B, the uninoculated seedlings receiving the Fe treatment had root lengths which were on average twice as long as those in the Mn + Zn treatment and 1.5 times longer than control roots (Figure 3B). For seed family C, the roots of uninoculated seedlings receiving Fe were twice as long as those of the inoculated seedlings receiving the other micronutrient treatments and 1.5 times longer than those of uninoculated control seedlings (Figure 3B).

The lengths of the roots ranging from 1.0 – < 1.5 mm diameter had significant differences between the uninoculated Fe treatment and the remaining micronutrient treatments of both the inoculated and uninoculated seedlings, whereby root lengths within the uninoculated seedlings were roughly 28 %, 23 % and 41 % greater than in seedlings receiving the mixed, Mn + Zn and control treatments respectively (Figure 3C). In comparison with the inoculated seedlings, the root length in Fe supplemented uninoculated seedlings was around 50 % greater relative to that in the Mn + Zn and Fe treatments and 36% greater than the seedling roots in the micronutrient mix and control treatments (Figure 3C). Additionally, within this diameter class, the root lengths of uninoculated seedlings receiving Mn + Zn were roughly 22 % higher than the control, and 34 % and 37 % higher than the inoculated seedlings receiving the Mn + Zn and Fe micronutrient treatments respectively (Figure 3C).

There was a significant micronutrient-related increase in root length in the 1.5 – 2.0 mm diameter class of roots (Figure 3D). Here too, the roots of uninoculated Fe-treated seedlings were significantly longer than the control (48 %) and also significantly longer than the roots of the inoculated seedlings irrespective of micronutrient treatment (52 %, 60 %, 70 % and 56 %) compared with the controls (Mn + Zn, Fe and mixed micronutrient treatments) respectively. Additionally, both the Mn + Zn and mixed micronutrient treatments of the uninoculated seedlings showed a significant 47 % and 58 % increase in root lengths, compared with the inoculated seedlings receiving manganese and zinc and iron treatments respectively. Lastly, within the uninoculated seedlings, plants receiving the Mn + Zn treatment showed an approximate 30 % root length increase compared with control seedlings (Figure 3D).

There was no significant seed family × pathogen × micronutrient three-way interaction associated with the number of root tips in the < 0.5 or the 0.5 – < 1.0 mm diameter categories (Table 4). Additionally, none of the two-way interactions was statistically significant. For the < 0.5 mm diameter root tip number there was a significant seed family effect; however, for root tips in the 0.5 – < 1.0 mm

diameter category none of the terms was significant (Table 4). A *post hoc* analysis revealed that within the < 0.5 mm diameter category, seed family B had higher root tip numbers than seed family C.

Table 3: Results from a linear mixed-effects model applied to the root length data from *Agathis australis* under various treatments. The pathogen is *Phytophthora agathidicida.* Treatments are described in the text.

Dropped term	*L*	*Df*	*p*
< 0.5 mm diameter			
Round #1			
Family × *pathogen* × *micronutrient*	19.41	6	0.004 **
0.5 – < 1.0 mm diameter			
Round #1			
Family × *pathogen* × *micronutrient*	16.80	6	0.011*
1.0 – < 1.5 mm diameter			
Round #1			
Family × *pathogen* × *micronutrient*	3.79	6	0.705
Round #2			
Pathogen × *micronutrient*	19.69	3	< 0.001 ***
Pathogen × *family*	0.83	2	0.659
Micronutrient × *family*	3.85	6	0.696
Round #3			
Pathogen × *micronutrient*	19.97	3	< 0.001 ***
Family	3.35	2	0.186
1.5 – 2.0 mm diameter			
Round #1			
Family × *pathogen* × *micronutrient*	5.50	6	0.481
Round #2			
Pathogen × *micronutrient*	16.85	3	< 0.001 ***
Pathogen × *family*	1.19	2	0.549
Micronutrient × *family*	3.42	6	0.755
Round #3			
Family	1.29	2	0.524

Pathogen × *micronutrient*	16.95	3	< 0.001 ***

Note: Root length data (<0.5, 0.5 – <1.0mm, 1.0 – <1.5mm, 1.5 – 2.0 mm diameter).
L = likelihood ratio statistic, *Df* = degrees of freedom of the likelihood ratio statistic, *p* = *p* value where * $p < 0.05$, ** $p < 0.01$, *** $p < 0.001$.
Statistical significance was determined at $\alpha = 0.05$.

Table 4: Results from a generalised linear mixed model with negative binomial error distribution and log link applied to the root tip number data from *Agathis australis* under various treatments. The pathogen is *Phytophthora agathidicida.* Treatments are described in the text.

Dropped term	*L*	*Df*	*p*
< 0.5 mm diameter			
Round #1			
Family × *pathogen* × *micronutrient*	9.30	6	0.157
Round #2			
Pathogen × *micronutrient*	5.21	3	0.157
Pathogen × *family*	3.10	2	0.211
Micronutrient × *family*	9.64	6	0.141
Round #3			
Pathogen	0.31	1	0.573
Micronutrient	2.89	3	0.408
Family	7.10	2	0.029 *
0.5 – 1.0 mm diameter			
Round #1			
Family × *pathogen* × *micronutrient*	12.50	6	0.061
Round #2			
Pathogen × *micronutrient*	1.50	3	0.683
Pathogen × *family*	0.80	2	0.671
Micronutrient family	6.90	6	0.328
Round #3			
Pathogen	1.24	1	0.265
Micronutrient	2.10	3	0.569
Family	2.76	2	0.252

Note: Root tip number data (< 0.5, 0.5 – < 1.0 mm diameter).
L = likelihood ratio statistic, *Df* = degrees of freedom of the likelihood statistic, *p* = *p* value where * indicates $p < 0.05$.

Statistical significance was determined at $\alpha = 0.05$.

Re-isolation of Phytophthora isolates

Phytophthora agathidicida was re-isolated from approximately 28 % of the inoculated plants. *Phytophthora agathidicida* was not detected in any of the control inoculated plants. *Pythium* was detected on 5 % of the inoculated plants and 2 % of the control plants.

Discussion

The results from this study indicate that inoculation with *P. agathidicida* induced root damage and/or physiological changes that were associated with an upregulation in ETR starting nine weeks after inoculation (Figure 1). Additions of Fe, Mn + Zn and a mixed micronutrient treatment had no significant impact on the ETR or the root length of *A. australis* in the presence of *P. agathidicida* but were found to stimulate root growth in the absence of the pathogen (Figure 3). *Phytophthora agathidicida* did have an effect on the ETR of the seedlings; however, this was time dependent. Eleven weeks following inoculation and nine weeks after micronutrient application began, the ETRs of the inoculated plants were approximately 10 % higher than those of the uninoculated control plants. Another two weeks later, the ETR of the inoculated plants had increased again, by roughly 16 %, resulting in a 26 % stimulation compared with that in the uninoculated control plants (Figure 1). This delay in host response is plausible given the time delay in the infection becoming established before the effects on host physiology become measurable. These results indicate that an increase in the strength of the below-ground carbon sink through pathogen consumption of labile carbohydrates (sugars), together with pathogen-induced root damage, triggered an upregulation of photosynthesis in the seedlings. These physiological findings imply that *P. agathidicida* increases its host's below-ground carbon allocation to compensate for the increased metabolic costs for defence and repair of pathogen-induced root damage.

The results from the root length data indicate that fine roots > 0.5 mm and < 2.0 mm diameter represented the large majority of total root length (Figure 3). The root length of the pathogen-infected seedlings without micronutrient addition was not significantly lower than that in the uninoculated

control plants without micronutrient supply, indicating that the pathogen had not consumed a large amount of root biomass up to that point in time. The lack of a consistent fine root response pattern in the two smallest diameter classes indicates that micronutrients may not severely limit fine root expansion. However, our data shows that seed families vary in their responses, as indicated by some significant micronutrient effects relative to the control. For example, the mixed micronutrient treatment appeared to stimulate root growth in the uninoculated plants of seed family C in the smallest diameter class.

The stimulatory effect of Fe became more apparent within the larger fine root diameter classes (> 1 mm), where uninoculated Fe-treated seedlings had not only significantly greater root lengths than the control, but also in comparison with the inoculated seedlings regardless of the micronutrient treatment (Figure 3C and 3D). Also, Mn + Zn supply resulted in significantly longer roots in uninoculated than in inoculated plants. The lack of stimulatory effects of Fe and Mn + Zn on root growth of the inoculated seedlings suggests that increased availability of these micronutrients in host root tissue might increase pathogen growth at the expense of root elongation. Alternatively, pathogens may interfere with physiological processes related to nutrient allocation to root growth. This has been observed in *Fagus sylvatica*, where the biotrophically growing and aggressive pathogen *Phytophthora citricola* dramatically increased the root sink strength (Schlink, 2010) which is in line with our results. The authors concluded that resource allocation to the growing (carbon) root sink was driven by an increasing energy demand of the roots, associated with an upregulation of host genes involved in energy metabolism.

Together with the ETR data, our findings suggest that *P. agathidicida* impaired fine root functioning, resulting in reduced nutrient uptake. Our results further imply that increases in the below-ground carbon sink through the consumption of photosynthates, wound respiration and enhanced carbon allocation to defence-related processes, change the host's carbon sink-source relationship.

Since photosynthetic activity is sink-driven, this imbalance is likely to result in an increase in photosynthetic carbon uptake (Fatichi, Leuzinger, & Körner, 2014), which is supported by the increase in ETR seen in infected kauri plants (Figures 1 and 2). Our study therefore provides evidence that plant-pathogen interactions have significant influences on the carbon source/sink relationship of *A. australis*, with persistent infection undermining the long-term resilience of the tree owing to the need to consistently replace fine roots and allocate resources to pathogen defence. It is likely that the sink-

driven photosynthetic upregulation in infected plants would become more pronounced over time with rising rates of root infection, up to a point where the detrimental effects of *P. agathidicida* increasingly affect root functioning and plant primary metabolism. The cascading process of infection and photosynthetic upregulation may ultimately impair whole-plant physiology, leading to disease and death recognised as kauri dieback. These physiological dynamics are of direct interest for the recognition of kauri dieback and the gradient of decline across trees, which may show indications of upregulated photosynthetic activity in the early stages of infection before declining. Our study investigated the stress and photosynthetic responses of kauri seedlings after pathogen infection and demonstrates that such physiological changes can be detected prior to the emergence of visual disease symptoms. It is important to determine whether the photosynthetic upregulation observed in infected seedlings also occurs in mature trees affected by the disease, since this physiological response may prove vital for the recognition of kauri dieback decline in native forest ecosystems. Knowledge about such a pathogen-triggered physiological signal can support the interpretation of remote sensing, where remotely acquired imagery, including canopy colour and chlorophyll fluorescence measurements, is used to detect stress symptoms in forest canopies associated with infection by *P. agathidicida* (Meiforth, Buddenbaum, Hill, & Shepard, 2020).

Previous studies have noted the trophic interactions that occur between plant pathogens and their hosts, and the direct impact these can have on both the physiology of the host, leading to mortality, and the carbon economy of the host, through the consumption of below-ground carbon sources held by the plant (Oliva, Stenlid, & Martínez-Vilalta, 2014). This is especially relevant for biotrophic and hemi-biotrophic pathogens where carbon is directly depleted from living cells, thereby disrupting the carbon transport system of the host. This damage occurs over many years, causing a slow death of the host as well as creating an additional below-ground carbon sink, causing an imbalance in the photosynthetic activity of the plant (Oliva et al., 2014).

This compensatory effect seen in plants responding to pathogens is sometimes seen in plants responding to herbivory. *Phytophthora* pathogens are important consumers of plant foliage within forest ecosystems globally, including species that directly consume above- and below-ground parts of plants including large trees (Hansen, 2015). Above-ground grazing removes carbon and therefore alters source-sink relationships in plants. In some species, especially within grassland species such as *Panicum coloratum,* one of the main responses to herbivory is change in the root-shoot growth

ratio, as a means to promote compensatory growth, with plants allocating more resources towards root growth to reduce unnecessary energy expenditure and maintain shoot growth (McNaughton, 1983; Dyer et al., 1991).

With respect to the first hypothesis, our results indicate that infection with *P. agathidicida* did affect the ecophysiology in kauri seedlings but instead of the expected reduction in photosynthesis, we detected an upregulation in photosynthetic activity. Our second hypothesis assumed a beneficial effect of micronutrient addition on the resilience and tolerance of *A. australis* to *P. agathidicida*. However, our results remain inconclusive owing to the late expression of above-ground symptoms, suggesting the need for a longer timeframe for future studies. In relation to our third hypothesis, that the mixed micronutrient treatment would be most effective in boosting plant performance, our results indicate that foliar micronutrient addition has no effect on the development of the disease in the early stages.

There were no visual aboveground symptoms (resinous cankers or lesions) of *P. agathidicida* infection observed on the lower trunk/crown of any of the inoculated seedlings during the 12-week trial. This was not unexpected, as according to Bradshaw et al. (2020), these aboveground symptoms are usually only observed during the chronic phase of disease infection, and it generally takes several years after root infection occurs for visual symptoms to become present. While smaller trees will decline at a much faster rate, it is predicted that it would be longer than the 12-week timespan of this study. Our findings give us a better understanding of the physiological responses of kauri seedlings to the pathogen during the initial stage of pathogen infection and establishment.

The conditions under which this experiment was conducted would certainly favour infection, because of the constant warm temperatures of the glasshouse. Infection of the *A. australis* seedlings had started as *P. agathidicida* was successfully re-isolated; however, the disease had not yet progressed to a severe state by the end of the experiment, with the pathogen re-isolated from 28 % of root fragments plated at harvest. The recovery rate of *P. agathidicida* may have been influenced by the presence of *Pythium,* which grows more rapidly than *Phytophthora* species*,* therefore often obscuring it on the selective media (despite the use of hymexazol, which is toxic to *Pythium*), (Tsao & Guy, 1977). Khaliq, Hardy, White & Burgess (2018), found that eDNA techniques, including metabarcoding, were able to identify all 30 of the *Phytophthora* phylotypes used in the study, while traditional methods, including baiting and selective media only detected around seven types. Additionally, *Phytophthora* specimens tend to have a slow revival of oospores and chlamydospores (Khaliq et al,

2018), and this has potentially contributed to confounding the re-isolation of *P. agathidicida* in this experiment.

Our results indicate that a longer period of time before harvesting is required to show the full progression of disease impact through to the point of acute decline. Extending the length of this type of experiment may lead to a better understanding of the dynamics of the decline from fine root infection to the advanced collar-rot which results in tree mortality. Additionally, continuous measurements of the electron transport rate of *A. australis,* for a longer period of time, would help to establish if the magnitude of the up-regulatory effect increases, levels off, or reverses over time and would also allow us to link any temporal dynamics that may occur to the time of appearance of chronic symptoms of the disease.

Conclusion

Applied micronutrient treatments did not influence early kauri dieback disease development, with infection progressing irrespective of nutrient availability. The observed upregulation of photosynthetic activity indicates that *P. agathidicida* influences carbon allocation within its host and may act as an additional below-ground carbon sink, affecting the physiology and resource allocation of *A. australis*. As this host response occurred under conditions of light saturation, growth in deep shade in the natural habitat may prohibit photosynthetic upregulation and thus hasten disease development more significantly than seen here where seedlings could more readily afford carbon losses to root pathogens and expenditures on defence and repair. Further research into the physiological interactions of this plant pathosystem over longer time frames is urgently required to gain a greater understanding of the physiological responses of *A. australis* to *P. agathidicida* attack, especially regarding the drivers of disease expression within a diverse natural forest environment. Getting a grasp on those drivers will become increasingly important under future warming trends since kauri is drought-sensitive and more frequent drought conditions may thus increase the risk of infection. Shedding light on the host-pathogen interactions and the underlying physiological processes is key to understanding kauri dieback disease and differentiating “disease-risk” from “pathogen-risk”. In this way, “disease-impacts” within landscapes can be evaluated through baseline and temporal monitoring of environmental drivers and metrics e.g. canopy physiology. Canopy thinning and decline represent

important indicators of the chronic phase of kauri dieback. Our study identified a canopy-physiological signal in response to root infection. This relationship may assist identifying the physiological precursors which indicate the transition of the disease from latency into its chronic phase.

Figure Legends

Figure 1: The light-saturated electron transport rate (ETR) of control and pathogen-infected *Agathis australis* seedlings from three seed families over 12 weeks post-inoculation.

The lowercase letters denote the results of a *post hoc* test. Different letters indicate statistically significant differences between the control and *Phytophthora agathidicida*-infected seedlings (PA group at each week) at $\alpha = 0.05$.

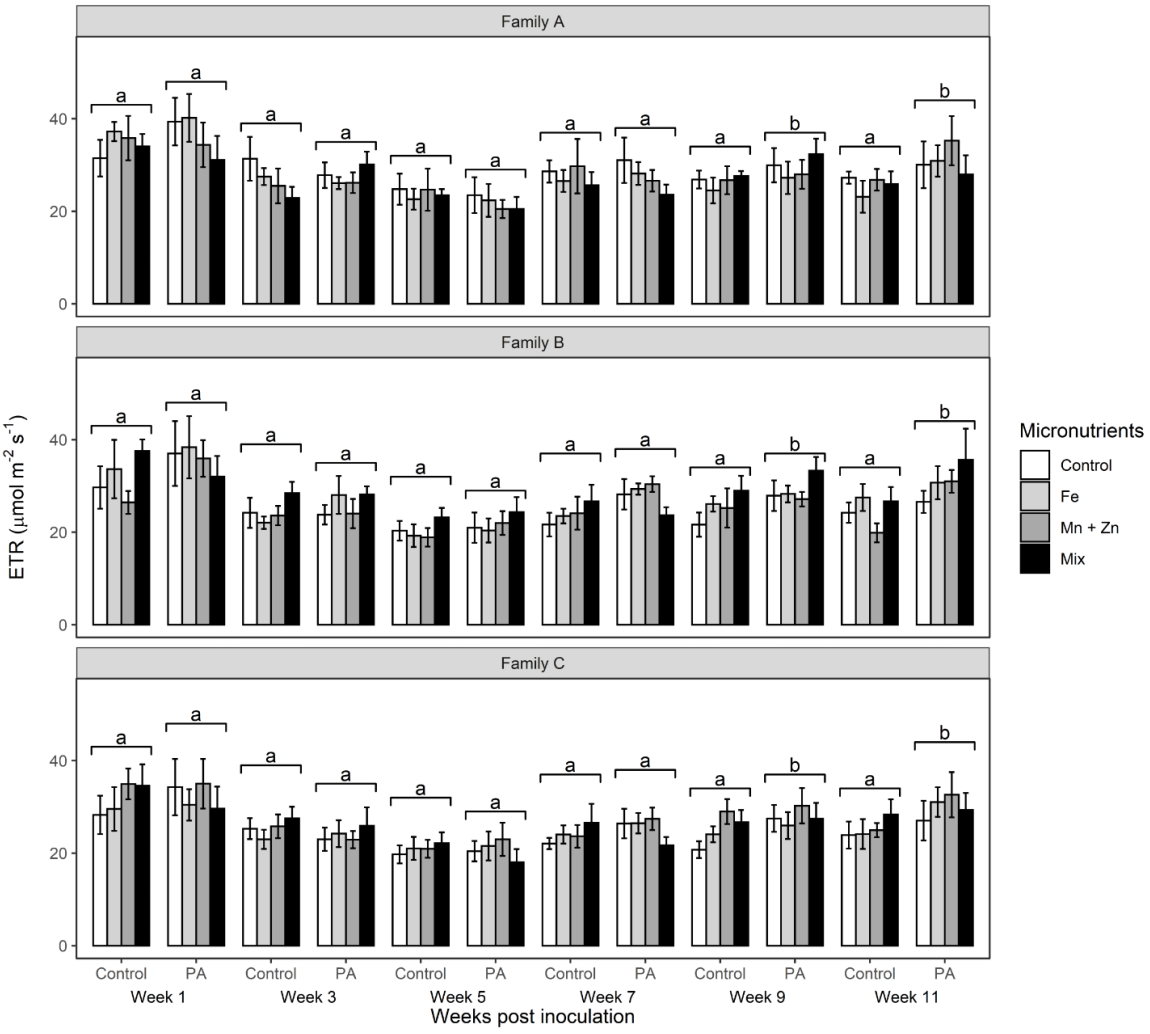

Figure 2: The estimated difference in the electron transport rate (ETR) between paired control and inoculated treatments of control and pathogen-infected *Agathis australis* seedlings over 12 weeks post-inoculation (ETR of the inoculated plants subtracted from the ETR of the control plants).

Error bars indicate 95 % confidence intervals of the model estimates of the treatment differences. If the confidence interval contains zero, the null hypothesis cannot be rejected at $\alpha = 0.05$. If the interval

does not contain zero, the null hypothesis can be rejected. This was supported by the statistical analysis for weeks 9 and 11. As a result of the multiplicity adjustment in the *post hoc* analysis, the difference observed 7 weeks after inoculation was not statistically significant.

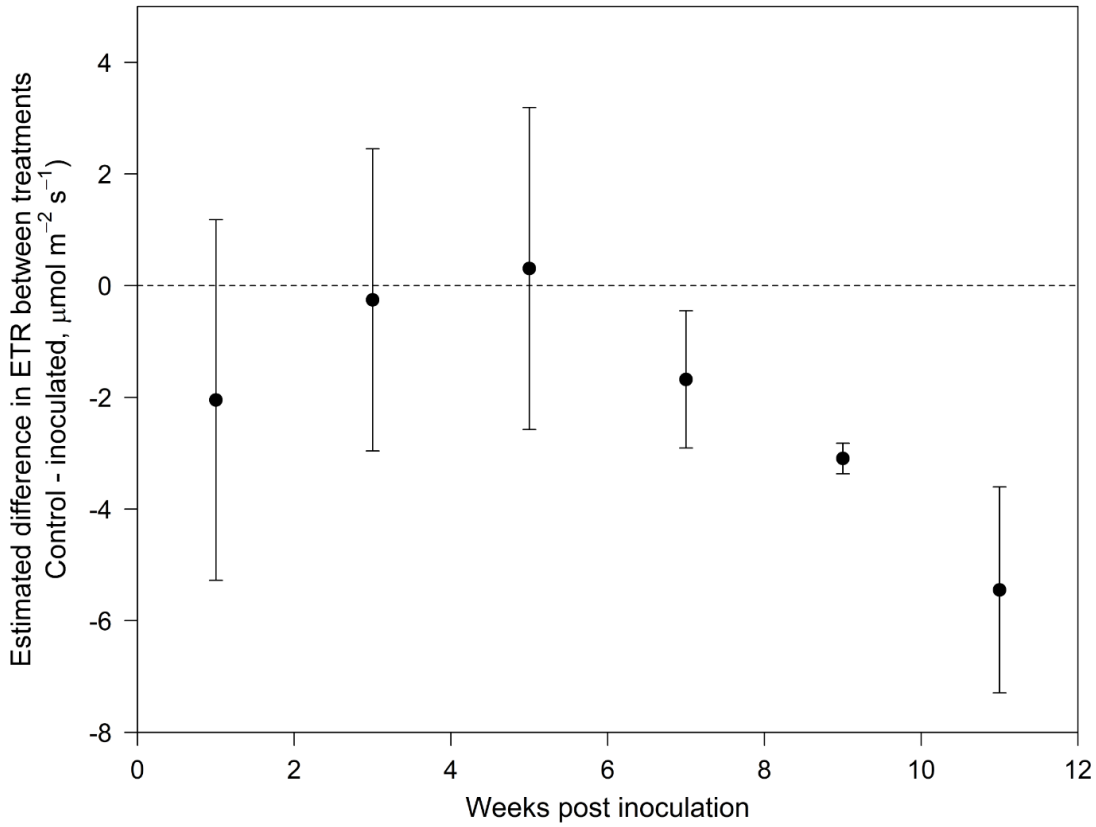

Figure 3: Root lengths of the control and pathogen-infected kauri (*Agathis australis*) seedlings by micronutrient treatment (and seed family) at the completion of the trial (12 weeks post-inoculation); (A) roots < 0.5 mm in diameter (B) roots 0.5 – <1.0 mm in diameter (C) roots 1.0 – <1.5 mm in diameter and (D) roots 1.5 – 2.0 mm in diameter.

Data in C and D were pooled across seed families because they had no significant effect on root length. The lowercase letters denote the results of a *post hoc* test, and different letters indicate statistically significant differences (α = 0.05) within the lowest level of nesting, *i.e.* only valid within the control or the pathogen-infected group in each figure panel.

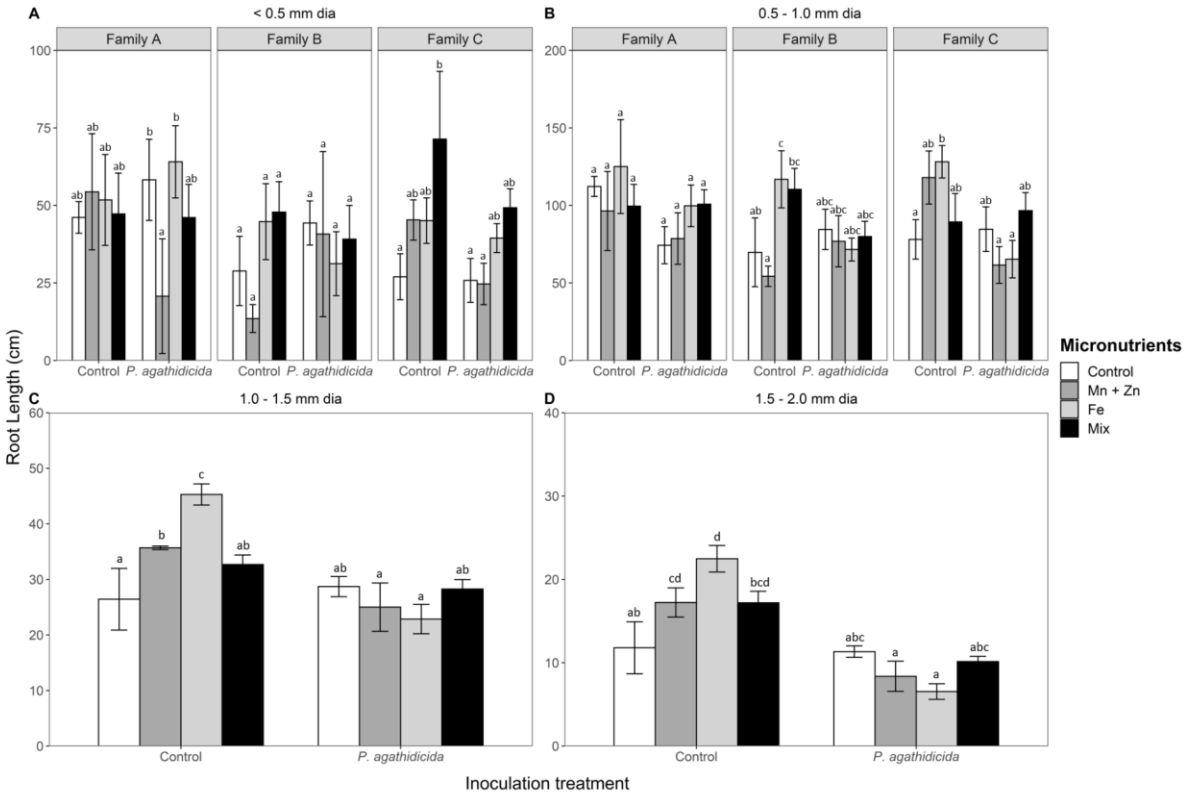

Acknowledgements

Funding for this research was provided by the Bioprotection Research Centre and Healthy Trees Healthy Future programme (Ministry of Business Innovation and Employment (C04X1305)). We would like to thank Scion, Manaaki Whenua – Landcare Research, and the Te Roroa Iwi trust board for supporting this work. We would also like to thank Dr C. Probst and Z. McGrath, from Manaaki Whenua - Landcare Research, St Johns, for assisting with laboratory work. Mention of commercial products in this manuscript is solely for the purpose of providing specific information on the constitutive ingredients.

References

Bader, M, K-F., & Leuzinger, S. (2019). Hydraulic coupling of a leafless kauri tree remnant to conspecific hosts. *iScience, 19,* 1238–1247. https://doi.org/10.1016/j.isci.2019.05.009

Bae, S. J., Mohanta, T. K., Chung, J. Y., Ryu, M., Park, G., Shim, S., ... & Bae, H. (2016). Trichoderma metabolites as biological control agents against Phytophthora pathogens. *Biological Control*, *92*, 128 – 138. https://doi.org/10.1016/j.biocontrol.2015.10.005

Bellgard, S.E., Pennycook, E.R., Weir, B.S., & Waipara, N.W. (2016). *Phytophthora agathidicida. Forest Phytophthoras, 6.* DOI: 10.5399/osu/fp.5.1.3748

Bellgard, S.E., Probst, C.M., Padamsee, M., Williams, N.M., & Weir, B.S. (2019). Kauri dieback screen and resilience; histopathological changes associated with New Zealand kauri roots due to infection with *Phytophthora agathidicida.* In: Bradshaw, R.E. and Horner, I.J. (Eds). *Abstract Proceedings from the New Zealand Plant Protection Society Phytophthora Symposium, 12 August 2019, Auckland, New Zealand,* pg 22.

Bradshaw, R.E., Bellgard, S.E., Black, A., Burns, B.R., Gerth, M.L., McDougal, R.L., … & Winkworth, R.C. (2020). *Phytophthora agathidicida*: research progress, cultural perspectives and knowledge gaps in the control and management of kauri dieback in New Zealand. *Plant Pathology, 69,* 3 – 16. https://doi.org/10.1111/ppa.13104

Brooks, M.E. Kristensen, K., van Benthem, K.J., Magnusson, A., Berg, W., Nielsen, W., Skaug, H.J., Maechler, M., & Bolker, B.M. (2017). GlmmTMB Balances Speed and Flexibility Among Packages for Zero-inflated Generalized Linear Mixed Modelling. *The R Journal, 9,* 379 – 400.

Dyer, M. I., Acra, M. A., Wang, G. M., Coleman, D. C., Freckman, D. W., McNaughton, S. J., & Strain, B. R. (1991). Source-sink carbon relations in two *Panicum coloratum* ecotypes in response to herbivory. *Ecology*, *72*, 1472–1483. https://doi.org/10.2307/1941120

Fatichi, S., Leuzinger, S., & Körner, C. (2014). Moving beyond photosynthesis: from carbon source to sink-driven vegetation modelling. *New Phytologist*, *201*, 1086–1095. https://doi.org/10.1111/nph.12614

Graham, R. D., & Webb, M. J. (1991). Micronutrients and disease resistance and tolerance in plants. *Micronutrients in agriculture, 2,* 329-370. https://doi.org/10.2136/sssabookser4.2ed.c10

Hansen, E.M. (2015). *Phytophthora* species emerging as pathogens of forest trees. *Current Forestry Reports, 1,* 16 – 24. https://doi.org/10.1007/s40725-015-0007-7

Horner, I.J., & Hough, E. (2014). Pathogenicity of four *Phytophthora* species on kauri in vitro and glasshouse trials. *New Zealand Plant Protection, 67,* 54 – 59. https://doi.org/10.30843/nzpp.2014.67.5722

Horsfall, J. G., & Dimond, A. E. (1957). Interactions of tissue sugar, growth substances, and disease susceptibility. *Zeitschrift für Pflanzenkrankheiten (Pflanzenpathologie) und Pflanzenschutz*, *64,* 415 – 421.

Jeffers, S.N. (2006). Identifying the species of *Phytophthora.* Retrieved from, https://fhm.fs.fed.us/sp/sod/misc/culturing_species_phytophthora.pdf

Khaliq, I., Hardy, G.E.St.J., White, D., & Burgess, T.I. (2018). eDNA from roots: a robust tool for determining *Phytophthora* communities in natural ecosystems. *FEMS Microbiology Ecology*, 94. DOI: 10.1093/femsec/fiy048Lenth, R. (2019). Emmeans: Estimated Marginal Means, aka Least-Squarāāes Means. R package version 1.3.2. https://CRAN.R-project.org/package=emmeans

Lerat, S., Lapointe, L., Gutjahr, S., Piché, Y., & Vierheilig, H. (2003). Carbon partitioning in a split-root system of arbuscular mycorrhizal plants is fungal and plant species dependent. *New Phytologist*, *157*, 589-595. https://doi.org/10.1046/j.1469-8137.2003.00691.x

Madgwick, H.A., Oliver, G., & Holten-Anderson, P. (1982). Above-ground biomass, nutrient and energy content of trees in a second-growth stand of *Agathis australis. New Zealand Journal of Forest Science, 12,* 3 – 6. Retrieved from, https://www.scionresearch.com/__data/assets/pdf_file/0009/59544/NZJFS1211982MADGWICK3-6.pdf

Manaaki-Whenua, Landcare Research. (2020). Ngā Harore o Aotearoa – New Zealand Fungi Database. Retrieved from, https://nzfungi2.landcareresearch.co.nz/default.aspx?NavControl=search&selected=NameSearch

Manter, D. K., Kelsey, R. G., & Karchesy, J. J. (2007). Photosynthetic declines in *Phytophthora ramorum*-infected plants develop prior to water stress and in response to exogenous application of elicitins. *Phytopathology*, *97*(7), 850-856. DOI:10.1094/ PHYTO-97-7-0850

McNaughton, S. J. (1983). Compensatory plant growth as a response to herbivory. *Oikos*, 329–336. DOI: 10.2307/3544305

Meiforth, J. J., Buddenbaum, H., Hill, J., & Shepherd, J. (2020). Monitoring of Canopy Stress Symptoms in New Zealand Kauri Trees Analysed with AISA Hyperspectral Data. *Remote Sensing*, *12*, 926. DOI:10.3390/rs12060926

Mittelstraß, K., Treutter, D., Plessl, M., Heller, W., Elstner, E. F., & Heiser, I. (2006). Modification of primary and secondary metabolism of potato plants by nitrogen application differentially affects resistance to *Phytophthora infestans* and *Alternaria solani*. *Plant Biology*, *8*(5), 653-661.

Morkunas, I., & Ratajczak, L. (2014). The role of sugar signalling in plant defense responses against fungal pathogens. *Acta Physiologiae Plantarum*, *36*, 1607-1619. https://doi.org/10.1007/s11738-014-1559-z

Nadeem, F., Asif Hanif, M., Majeed, M.I., & Mushtaq, Z. (2018). Role of macronutrients and micronutrients in the growth and development of plants and prevention of deleterious plant diseases- a comprehensive review. *International Journal of Chemical and Biochemical Sciences, 12*, 31–52.

National (Kauri dieback) Pest Management Plan Proposal. (2019). Retrieved from https://www.kauridieback.co.nz/media/1901/npmp-proposal-for-consultation-18022019.pdf

Oliva, J., Stenlid, J., & Martínez-Vilalta, J. (2014). The effect of fungal pathogens on the water and carbon economy of trees: implications for drought-induced mortality. *New Phytologist*, *203*, 1028–1035. https://doi.org/10.1111/nph.12857

Padamsee, M., Johansen, R. B., Stuckey, S. A., Williams, S. E., Hooker, J. E., Burns, B. R., & Bellgard, S. E. (2016). The arbuscular mycorrhizal fungi colonising roots and root nodules of New Zealand kauri *Agathis australis*. *Fungal biology*, *120*, 807-817. https://doi.org/10.1016/j.funbio.2016.01.015

Pinheiro, J., Bates, D., DebRoy, S., Sarkar, D., & R Core Team. (2018). _nlme: Linear and Nonlinear Mixed Effects Models_. R package version 3.1-140, <URL: https://CRAN.R-project.org/package=nlme>.

Peterson, P.J. (1963). The occurrence of Rhodoxanthin in red leaved seedlings of *Agathis australis.* *Journal of Experimental Botany, 14,* 1 – 9. https://doi.org/10.1093/jxb/14.1.1

R Development Core Team. (2016). R: *A language and Environment for Statistical Computing*. R Foundation for Statistical Computing. Vienna, Austria.

Rengel, Z. (1999). Mineral nutrition of crops: Fundamental mechanisms and implications. In Z. Rengal (ed.) *Mineral Nutrition of Crops: Fundamental Mechanisms and Implications* (pg 15 – 20). CRC Press.

Rolfe, S. A., & Scholes, J. D. (2010). Chlorophyll fluorescence imaging of plant–pathogen interactions. *Protoplasma, 247*, 163–175. DOI 10.1007/s00709-010-0203-z

Scharte, J., Schön, H., & Weis, E. (2005). Photosynthesis and carbohydrate metabolism in tobacco leaves during an incompatible interaction with *Phytophthora nicotianae. Plant, Cell & Environment, 28*, 1421–1435

Schlink, K. (2010). Down-regulation of defense genes and resource allocation into infected roots as factors for compatibility between *Fagus sylvatica* and *Phytophthora citricola*. *Functional & integrative genomics*, *10*, 253-264. https://doi.org/10.1007/s10142-009-0143-x

Schnabel, G., Strittmatter, G., & Noga, G. (1998). Changes in photosynthetic electron transport in potato cultivars with different field resistance after infection with *Phytophthora infestans*. *Journal of Phytopathology*, *146*, 205-210.

Scott, P., Bader, M. K. F., Burgess, T., Hardy, G., & Williams, N. (2019). Global biogeography and invasion risk of the plant pathogen genus *Phytophthora*. *Environmental Science & Policy*, *101*, 175-182. https://doi.org/10.1016/j.envsci.2019.08.020

Scott, P., & Williams, N. (2014). *Phytophthora* diseases in New Zealand forests. *NZ Journal of Forestry, 59.*

Shilton, B. D. (2017). *The effect of plant hormones on phenolic production in Kauri trees* (Doctoral dissertation, Auckland University of Technology).

Steward, G.A., & Beveridge, A.E. (2010). A review of New Zealand kauri (*Agathis australis* (D.Don) Lindl.): its ecology, history, growth and potential for management for timber. *New Zealand Journal of Forestry Science, 40*, 33–59.

Tsao, P.H., & Guy, S.O. (1977). Inhibition of *Mortierella* and *Pythium* in a *Phytophthora*-isolation medium containing hymexazol. Phytopathology, 67, 796 – 801.

Vettraino, A.M., Natili, G., Anselmi, N., & Vannini, A. (2001). Recovery and pathogenicity of *Phytophthora* species associated with a resurgence of ink disease in *Castanea sativa* in Italy. *Plant Pathology, 50,* 90–96. https://doi.org/10.1046/j.1365-3059.2001.00528.x

Waipara, N., Hill, S., Hill, L., Hough, E., Horner, I. (2013). Surveillance methods to determine tree health, distribution of kauri dieback disease and associated pathogens. *New Zealand Plant Protection, 66,* 235 – 241. https://doi.org/10.30843/nzpp.2013.66.5671

Wyse, S.V., Burns, B.R., & Wright, S.D. (2014). Distinctive vegetation communities are associated with the long-lived conifer *Agathis australis* (New Zealand kauri, Araucariaceae) in New Zealand rainforests. *Austral Ecology, 39,* 388–400. https://doi.org/10.1111/aec.12089